ELSEVIER

1 January 2000

Optics Communications 173 (2000) 389–395

OPTICS COMMUNICATIONS

www.elsevier.com/locate/optcom

Guided-light two-wave-mixing on a spherical surface

Stefano Sottini *, Emilia Giorgetti, Alessandro Gignoli, Luca Palchetti, Daniela Grando

Istituto di Ricerca sulle Onde Elettromagnetiche ''Nello Carrara'', Via Panciatichi 64, 50127 Florence, Italy

Received 12 August 1999; accepted 5 October 1999

Abstract

A novel guided structure is proposed which is aimed at developing integrated all-optical signal processors exploiting two wave mixing interactions. The structure is based on the whispering propagation on a hemispherical glass substrate and contains a dye-doped photoresist film as the test nonlinear material. Its functionality was demonstrated successfully with two wave mixing experiments that were performed with CW light at 1321 nm and with a probe beam at 647 nm.

PACS: 42.79.Hp; 42.65.Hw; 42.82.Bq; 42.65.Wi
Keywords: Two wave mixing; Whispering propagation; All-optical signal processing

1. Introduction

The development of ultrafast all-optical integrated devices based on third order nonlinear effects is actively being pursued [1]. For this purpose, it is important to prepare and test novel materials with large and fast nonlinearities and to make them compatible with guided structures. Indeed, the insertion of nonlinear materials into integrated optical circuits often represents a challenge, due to their non-optimized optical quality (for example dishomogeneity, small thickness, and high propagation losses). Moreover, the nonlinear characterization of such materials is a crucial point: it has to be performed in the same conditions as for a real device, that is with guided light. As a consequence, the design of suitable device-architectures is required in order to facilitate the nonlinear characterization, to exploit thoroughly the material nonlinear properties and to reduce the above mentioned drawbacks related to guided propagation. In this sense, the degenerate four wave mixing (DFWM) technique compares quite well with other alternatives as Z-scan, self-phase-modulation, nonlinear coupling, etc., not only for material characterization, but also for device design [2,3]. Here, an unconventional architecture is proposed, which permits the testing of nonlinear films with different DFWM configurations and exhibits potentialities to develop an integrated device.

2. Device design and experimental tests

The best known DFWM geometry consists of two counterpropagating pump beams and an off-axis

* Corresponding author. Tel.: +39-055-42351; fax: +39-055-410893; e-mail: sottini@iroe.fi.cnr.it

0030-4018/00/$ - see front matter
PII: S0030-4018(99)00602-1

probe. This interaction produces a fourth beam that, under suitable approximations, is the phase-conjugate of the probe [4]. A special case of DFWM, which is particularly interesting in view of the development of all-optical AND gates [5] is the two wave mixing (TWM): in this case, the two pumps propagate in almost the same direction (the angle in between is typically $< 1^{\circ}$), create a real time spatial grating and generate new beams by self-diffraction. The development of integrated devices based on DFWM interactions is not straightforward: indeed, all the optics that is necessary to produce the nonlinear interaction must be integrated on a single substrate and all the input and output beams must be efficiently coupled with channel guides or optical fibers. Moreover, the mixing process inside a third order nonlinear material is inherently not compatible with channel waveguides because, according to the current picture of dynamic gratings, a significant efficiency can be obtained only if the width of the mixing beams is large enough to contain several fringes, that is at least 100 μm. Here a novel architecture is proposed which complies with the previous requirements of integration, compactness and efficiency.

The device is based on a hemispherical glass substrate. The whispering gallery mode propagation combined with Fermat's principle allows a point light source at the hemisphere edge to be perfectly collimated on the top of the hemisphere and refocused at the diametrically opposite point [6]. If a thin strip of a nonlinear film is fabricated along a meridian, just on the top of the hemisphere, it can be used for DFWM or TWM tests as shown in Fig. 1. In the figure, where a top view of the hemisphere is sketched, O_1 and O_2 are the input pumps: they are collimated after whispering propagation along the surface of the first quarter of sphere, then they mix in the nonlinear film and generate two self-diffracted beams, which are focused at N_3 and N_4. The spherical geometry allows, if necessary, the addition of a third beam (that can be either co- or counter-propagating) coming from source P and schematically represented in Fig. 1 by the bold lines. This probe beam, that can be at a different frequency, is also diffracted by the real time grating and produces two new beams focused at P_1 and P_2, while its undiffracted part is imaged at P_0. The angles γ and ψ,

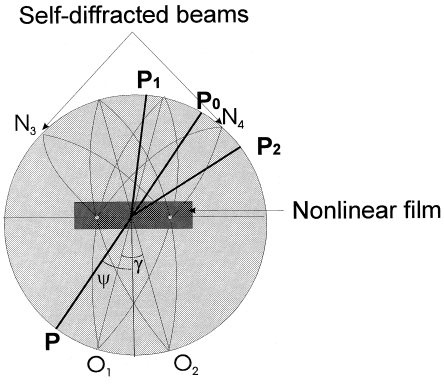

Fig. 1. Top view of the proposed device.

which characterize the mixing geometry, can be easily varied by moving the sources O_1, O_2 and P along the edge of the hemisphere. It is noticeable that the largest part of the optical path is in glass so reducing the absorption problems, while the nonlinear interaction length, that is limited by the width of the film strip, can be easily optimized to prevent phase-mismatch and to achieve a good trade-off between losses and mixing efficiency.

Some preliminary experiments, that demonstrate the working principle of the hemispherical TWM device, have been carried out on a BK7 glass hemisphere of radius $R = 8.87$ mm. A thin nonlinear film was deposited by spin coating on the top of this substrate. The nonlinear material was a saturable absorber, Kodak 14617 bis (4-diethylaminodithiobenzil) nickel dissolved in 1813 Microposit photoresist: the dye strongly absorbs between 900 and 1400 nm and consequently exhibits a large thermo-optic nonlinearity. Of course, this material is not suitable for fast devices, but can be used conveniently as a demonstrator: continuous wave could be used and the dye absorption problems could be limited by using short propagation lengths (the strip was 500 μm wide) and by controlling the film throughput by varying the dye concentration in the photoresist matrix.

The dye powder was dissolved in the photoresist with a concentration of 2.2 g/l; then, the solution was spun on the top of the hemispherical substrate at a speed of 4000 rpm for 30 s, in order to achieve a film thickness of 1.1 μm. Lastly, most of the film

was removed by UV irradiation through a mask and subsequent development. As a result of this process, a 10 mm-long and 0.5 mm-wide film strip was deposited along a meridian on the top of the hemisphere (Fig. 1): as shown in Fig. 2, its 0.5 mm width included the tapered edges [7]. These tapers were obtained simply by keeping the mask at a distance of 42 mm from the sample during the UV irradiation. Since the extinction coefficient of the dye at 1321 nm is 0.5×10^4 l mol.$^{-1}$ cm^{-1}, the losses induced by film crossing were estimated to be ≈ 7 dB/mm. A dye doped photoresist film was spun from the same solution on a microscope glass slide in the same conditions; its nonlinearity was measured at 1321 nm with a CW diode pumped Nd:YLF laser by means of a nonlinear grating coupling experiment [8] and was $n_2 = 2 \times 10^{-10}$ m^2/W with a 28% experimental error.

A huge number of whispering gallery modes (> 1000) can be supported by the spherical glass substrate used in our experiments; however, we evaluated that, at 1321 nm, the coupling efficiency between a commercial 10/125 single mode fiber and the fundamental whispering mode $m = 0$, $l = 0$ is larger than 40%. On top of the hemisphere, the nonlinear film is also present and the structure becomes a curved waveguide. In general, at its input edge, the incoming fundamental whispering mode couples into those modes supported by the new structure that have radial field distribution $m_g = 0_g$, ... n_g and the same lateral field distribution, that is mode-index $l = 0$, which, here as follows, will be neglected. With our experimental parameters, at 1321 nm, the incoming whispering mode splits into two radial modes, 0_g and 1_g that are shown in Fig. 3, where ρ is the radial coordinate. As illustrated by the figure and summarized in Table 1, the power percentage P_f confined inside the film is large only for the 0_g mode, while the 1_g mode mainly propagates inside the substrate: indeed, from calculations it results that P_f is 85% and 0.01% for the two modes, respectively. Unfortunately, and particularly

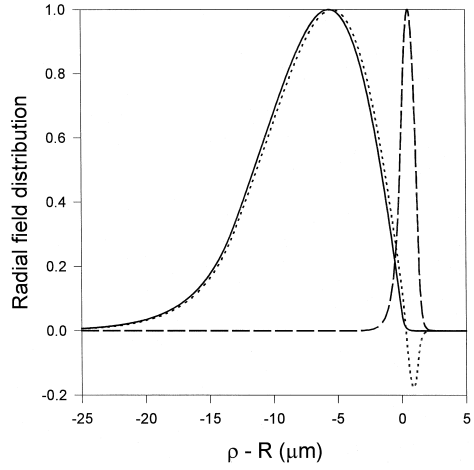

Fig. 3. Theoretical radial field distributions at 1321 nm of the $m = 0$, $l = 0$ whispering mode of the glass hemisphere (continuous line) and of the $m = 0_g$, $l = 0$ mode (dashed line) and of the $m = 1_g$, $l = 0$ mode (dotted line) of the curved waveguide containing the dye-doped photoresist film.

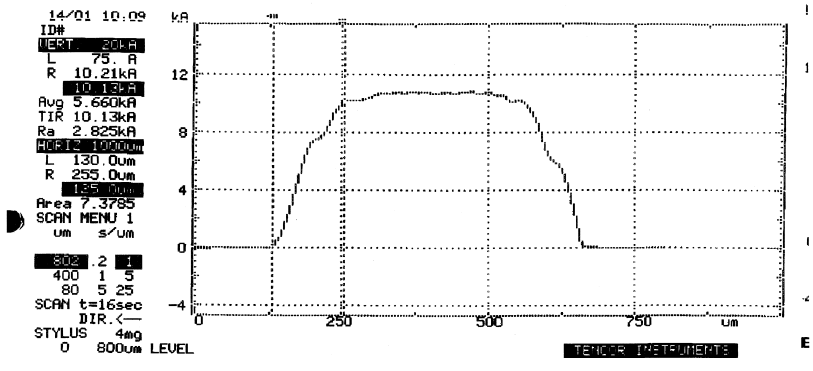

Fig. 2. Profile of the dye-doped photoresist film obtained with a stylus profilometer.

Table 1
Modal structure of the curved waveguide at pump and probe wavelengths

Wavelength (nm)	Mode index m_g	P_f (%)	η_c (%)
647	0_g	97	7
	1_g	82	27
	2_g	< 0.1	–
	3_g	< 0.1	–
	4_g	< 0.1	–
1321	0_g	85	12
	1_g	0.01	79

in the case of a film with sharp edges, it is to be expected that the coupling of the incoming light into the 1_g mode were favoured by the much better overlap with the original whispering mode $m = 0$ (also depicted in the figure) at the expense of the more confined 0_g mode. However, the coupling efficiency η_c into the 0_g mode can be increased by properly tapering the film input edge in order to modify adiabatically the field distribution and match the 0_g mode as closely as possible [7]. As also reported in Table 1, we calculated that, at 1321 nm, the input tapered edge of our film, that is shown in Fig. 2, permits to achieve 12% and 79% coupling efficiencies into the 0_g and 1_g modes, respectively, so that, as a whole, 10.3% of the input radiation propagating in the fundamental whispering mode can actually be confined inside the dye-doped layer. Taking into account that a symmetrical behaviour is expected at the film output edge, where the 0_g and 1_g modes merge again into the fundamental whispering mode of the glass sphere and that the throughput of the dye-doped photoresist film was 45%, it can be concluded that only 0.5% of the light detected at the hemisphere output had actually crossed the nonlinear film. However, it is to be noted that even if this poor efficiency made the TWM tests more difficult, it is not inherent to the geometry of the device: indeed, it is essentially due to the depth of the $m = 0$, $l = 0$ whispering mode that, with our sphere radius and index of refraction was 13 μm at 3 dB, to be compared with the film thickness, that was only 1.1 μm. Smoother tapers at the film edges and a better confinement of the input radiation that is achievable by fabricating a waveguide on the spherical substrate can increase this percentage up to 50% [7].

Coming back to the performance of our device, the expectations above outlined resulted to be in agreement with the results of some linear tests carried out on the hemisphere before and after the deposition of the nonlinear film. A low power laser beam at 1321 nm was coupled to the hemisphere through a 10/125 monomode fiber. The variations observed between the output intensity distributions before and after film deposition were negligible and consistent with the estimation that only a small amount of the guided energy actually travelled inside the photoresist doped film. Moreover, the wide spreading of the intensity distribution along the radial direction in both cases, suggested a large amount of scrambling among higher order modes, due to both field mismatch and to scratches and irregularities at the edge of the substrate.

Nonlinear tests were performed by using the TWM geometry depicted in Fig. 1. The radiation at 1321 nm was split into two beams which were focused and coupled to the hemisphere edge so that point sources O_1 and O_2 were 50 μm apart. As a consequence, the angle γ between the pump beams was 5.6 mrad. The width of such beams in the nonlinear film was ≈ 2.8 mm and the period Λ of the resulting grating was 154 μm. The intensity distribution obtained at the output edge is shown in Fig. 4(a): no evidence of the self-diffracted beams could be detected at N_3 and N_4. As a matter of fact, according to our calculations, and taking into account that the maximum power available from the Nd:YLF laser was 100 mW, the power per pump confined in the nonlinear film could not exceed 2 mW, which corresponds to a diffraction efficiency η of the order of 1% [9]. As a consequence, the expected intensity of the diffracted signals at the output was $\approx 10^{-4}$ times smaller than that of the pump beams because the largest part of the guided light did not cross the nonlinear material. Thus, the noise surrounding the pump spots in Fig. 4(a), prevented us from detecting such a small self-diffracted signal. However, the existence of a real time grating could be demonstrated, as shown in Fig. 1, by adding a weak probe beam at a different wavelength, that co-propagated with one of the pumps.

The probe beam came from an Ar–Kr laser ($\lambda =$ 647 nm) and was focused at the input point P. At this wavelength, and neglecting again the mode index l

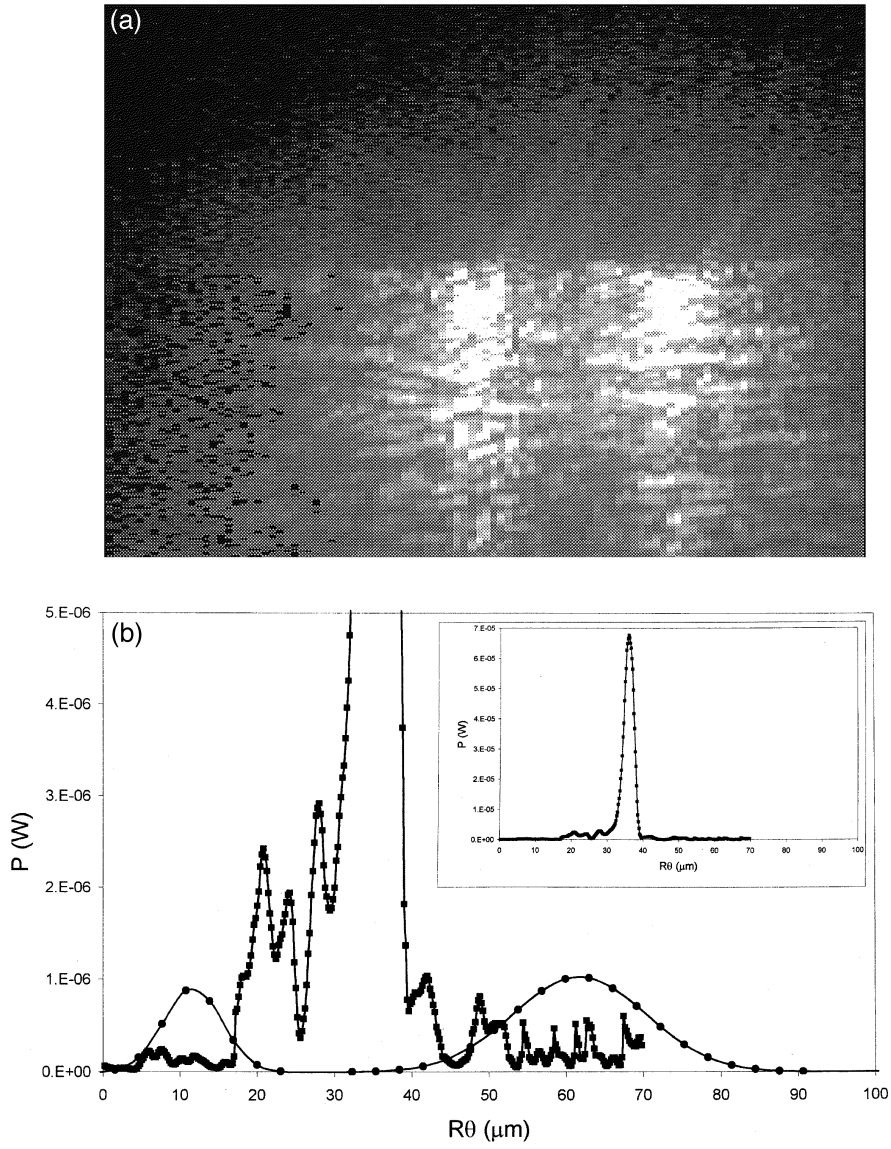

Fig. 4. (a) Intensity distribution at the hemisphere output during a TWM experiment. The image was registered with an IR video camera; and (b) typical ± 1-order diffracted signals (circles) produced by reading the real time grating with a probe beam at 647 nm and obtained after filtration and subtraction of the 0-order contribution (squares). $R\theta$ is the linear coordinate along the hemisphere edge. For the clarity of the figure, the vertical scale was cut: the complete 0-order distribution is reported in the inset.

associated with the lateral field distribution, the curved structure formed by the BK7 substrate and the polymer layer supports 5 modes (Table 1). In the case of the $m = 0_g$, 1_g modes 97% and 82% of the power, respectively, is confined inside the film; in contrast, for the $m = 2_g$, 3_g, 4_g modes this value is lower than 0.1%, so that these modes cannot contribute to the diffracted signal. The coupling efficiencies η_c produced by the film tapered junction between the fundamental whispering mode of the glass

hemisphere and the $m = 0_g$, 1_g modes of the curved waveguide, at this wavelength, were 7% and 27%, respectively, so that a 29% power percentage could be actually transferred inside the polymer film and a 8% power percentage left it after interaction with the real time grating.

The use of the probe strongly alleviated the detection problems because the pump noise could be reduced by the use of a band pass filter and diffraction efficiencies η of the order of several % could be obtained. Typical experimental results are shown in Fig. 4(b): the squares represent the intensity distribution of the probe beam at the hemisphere output when the infrared pumps are off and the circles represent typical ± 1-order diffracted signals of the probe beam. The diffracted beams were obtained from the output signal registered with the infrared pumps on after subtraction of the 0-order contribution. For the clarity of the figure, the vertical scale was cut and the complete 0-order distribution is reported in the inset. By taking into account that only 8% of the red light collected at the hemisphere output had crossed the polymer film and by comparing the intensities of the peaks shown in Fig. 4(b), we estimated that the diffraction efficiency of the probe was actually 18%. Under the assumption that the nonlinear refractive index modulation at 647 nm was the same as observed at 1321 nm and that the film absorbence at 647 nm was negligible, this value was consistent with the quasi-normal incidence of the probe beam on the real time grating ($\psi \approx 0°$).

3. Conclusions

In conclusion, a new architecture was described, which is suitable to test nonlinear films with different DFWM configurations. This architecture minimizes the effects of both linear and nonlinear absorption mechanisms and exhibits a high degree of integration and compactness. It is based on the whispering propagation on the surface of a hemispherical glass substrate and on a film strip made of a nonlinear material, which is laid on the top of the hemisphere. Some preliminary tests carried out by using a photoresist film doped with a saturable absorber confirmed our expectations. The problems we met, namely low efficiency and noise, were related to the small percentage of the guided radiation confined in the nonlinear film and to a large amount of in-plane scattering produced at the film edges. These problems were not inherent to the proposed configuration: indeed, up to 50% of the guided light could be transferred into the nonlinear film if the film tapered edges were properly shaped and a waveguide were fabricated onto the glass substrate (i.e. by ion-exchange) in order to increase the power confinement at its surface. Alternatively, efficient light transfer into the nonlinear material can be obtained by replacing the spun film with a groove filled with the nonlinear material particularly in those cases when the solubility of the nonlinear medium is poor and/or the film patterning is not straightforward as with photoresist host matrices [10].

An interesting advantage of this architecture is that optical fibers can be easily coupled to the device [6]. In case, the hemisphere could be substituted by a geodesic lens [11] so producing a planar geometry, which can favour the light coupling with channel waveguides. Taking also into account that cheap techniques for replication of microoptic components are in quick progress, the proposed architecture seems to have potential for the development of devices for practical applications.

Acknowledgements

This research was partially funded by the Italian Targeted Project on Advanced Materials for technological Applications MSTAII.

References

[1] G.I. Stegeman, W.E. Torruellas, Phil. Trans. R. Soc. London A 354 (1996) 745–756.
[2] C. Malouin, A. Villeneuve, G. Vitrant, P. Cottin, R.A. Lessard, J. Opt. Soc. Am. B 15 (1998) 826–837.
[3] E. Giorgetti, Proc. of the Intern. Conf. on Laser '98, Tucson (Az), 7–11 December 1998 (1999) 653–660, and references therein.
[4] Y.R. Shen, The Principles of Nonlinear Optics, New York, 1984 (Chapter 15).
[5] P. Horan, W. Blau, H. Byrne, P. Berglund, Appl. Opt. 29 (1990) 31–36.

[6] S. Sottini, E. Giorgetti, C. Marcellino, Pure Appl. Opt. 1 (1992) 359–372.
[7] S. Sottini, D. Grando, L. Palchetti, E. Giorgetti, IEEE J. Quantum Electron. 31 (1995) 1123–1130.
[8] G. Assanto, M.B. Marques, G.I. Stegeman, J. Opt. Soc. Am. B 8 (1991) 553–561.
[9] E. Giorgetti, P. Lambkin, Q. Li, L. Palchetti, S. Sottini, D. Grando, W. Blau, J. Opt. Soc. Am. B 12 (1995) 58–66.
[10] E. Giorgetti, G. Margheri, L. Palchetti, S. Sottini, M. Mennig, Appl. Phys. B 67 (1998) 587–591.
[11] S. Sottini, E. Giorgetti, J. Opt. Soc. Am. A 4 (1987) 346–351.